Electronic Supplementary Material (ESI) for Chemical Communications.

ELECTRONIC SUPPLEMENTARY INFORMATION

Organic alloys of room temperature liquids thiophenol and selenophenol

Sajesh P. Thomas, R. Sathishkumar and T. N. Guru Row*

1. *In situ* cryocrystallization experiments:

Commercially available (Sigma Aldrich) samples of thiophenol and selenophenol were used for crystal growth as received. The experimental setup consists of a 3-circle Bruker Apex II X-ray diffractometer with an attached low-temperature OXFORD N_2 cryosystem device for cooling the sample. The N_2 cryojet is arranged with positional flexibility to scan over the entire area of the capillary in order to achieve zone melting and re-cooling of the sample. The liquid sample was loaded into a Lindemann glass capillary (0.3 mm diameter), and the capillary was then flame sealed at both the ends. The sample was cooled slowly in the capillary until it just solidified, monitored by using video camera connected to the computer. Melting and recrystallization of the sample were repeated by moving the tip of N_2 cryojet, until a satisfactory domain was obtained. In case of solid solutions, the samples of thiophenol and selenophenol were mixed thoroughly before filling into the capillary. The software RLATT in the Bruker software suite has been used for the determination of unit cell parameters from periodically arranged arrays of the lattice points (reflections). 1: 1, 1:2 and 1:3 mixtures of selenophenol and thiophenol were used for generating alloy phases. These liquids were mixed in their volume ratios and thoroughly mixed via sonication, before filling into a capillary tube. The liquid was cooled to freeze and melted for obtaining good and uniform crystal domains. A special care is taken during the cell indexing to make sure that selenophenol and thiophenol crystal phases do not exist as separate domains and leading to average structure (using RLATT). It should be noted that, though several attempts were made to obtain crystalline domains of phenol-thiophenol mixtures and phenol-selenophenol mixtures, they all resulted in glassy/amorphous domains as became evident from their diffraction patterns.

2. Crystal structure refinement

The structures were solved and refined using SHELX97 module in the program suite WinGX. The geometric calculations were carried out by PARST95 and PLATON. Molecular diagrams were generated using ORTEP-3 and the packing diagrams with Mercury 2.3.

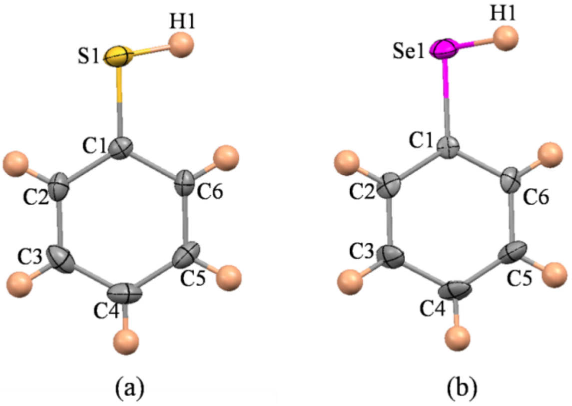

Figure S1. ORTEP projections of thiophenol and selenophenol plotted normal to the aromatic plane with 50% probability ellipsoids and the atom numbering scheme.

In the structure refinement, all aromatic protons were geometrically fixed. In thiophenol, the S–H proton was identified from difference Fourier map and fixed to using DFIX command the S–H distance of 1.338 Å, obtained from neutron diffraction. In the case of selenophenol, the Se–H distance of 1.45 Å reported based on a geometrical optimization calculation was used (Sladek, V.; Rottmannová, L.; Škorňa, P.; Ilčin, Michal; Lukeš, V. *Acta Chimica Slovaca* **2012**, *5*, 159-163.). Crystal structures of thiophenol, selenophenol and their solid solutions (selenophenol: thiophenol; 5:95, 9:91, 25:75 and 43:57) are described here. ORTEP projections are given in Figure S2.

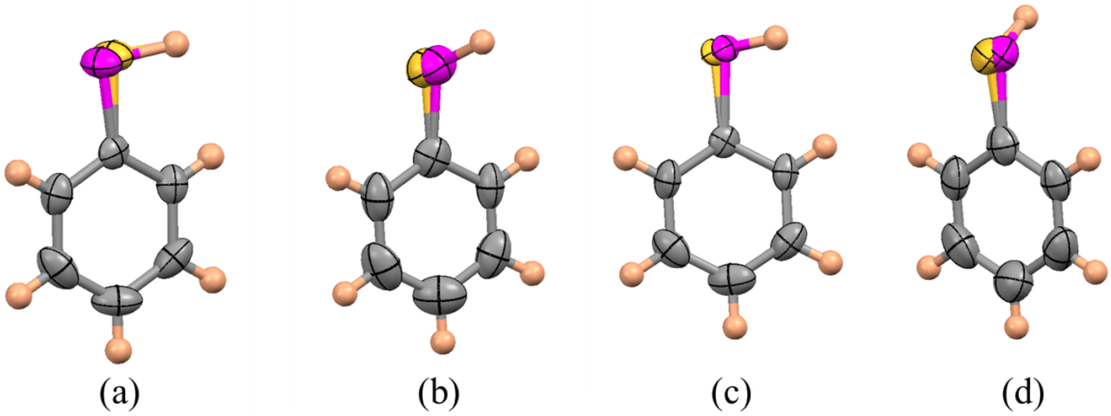

Figure S2. ORTEP projections of selenophenol: thiophenol alloys with 50% probability ellipsoids representing (a) 5 %, (b) 9%, (c) 25% and (d) 43% alloy phases.

Crystal structure refinement strategy for solid solutions:

The structural models of the solid solutions of thiophenol and selenophenol were constructed taking into account of two features; (i) Variable occupancies of S and Se atoms that add up to one, (ii) though thiophenol and selenophenol form solid solutions, unlike the cases of many inorganic structures, here S and Se atoms cannot occupy same crystallographic positions as the C−S and C−Se bond lengths are slightly different (iii) the occupancies of S and Se atoms can be correlated with their thermal parameters, thermal parameters of the C atoms and the presence of H atoms in the model.

After attempting several refinement methods, the following strategy have been used for the stepwise refinement of the models:

(i) model with the phenyl ring and S atom is refined with full occupancy on S atom.

(ii) Se position is located from the difference Fourier map and the occupancies of S and Se were refined freely.

(iii) the resulting occupancy value of S is used as the initial value of occupancy free variable (FVAR) in the next step of refinement using PART command (with S in part1 and Se in part2)

(iv) the converged values of S and Se occupancies are fixed for the next step of refinement as the anisotropic thermal parameters of C atoms are refined, keeping S and Se isotropic.

(v) hydrogen atoms are located from the difference Fourier map and refined.

(vi) with H atoms and anistropic C atoms in the model, the occupancies of S and Se are refined again using PART command (with S in part1 and Se in part2). The isotropic thermal parameters of S and Se atoms are restrained to be equal by EADP command during the refinement.

(vii) fixing the converged values of S and Se occupancies, anisotropic thermal parameters of S and Se atoms are refined.

Converged occupancy free variables (FVAR for S atom occupancy) for the 5%, 9%, 25% and 43% alloys are 0.95432, 0.90780, 0.74957 and 0.56817 respectively.

The details of crystal structure solution and refinement are given in Table 1. The intermolecular interactions are listed in Table 2.

Table S1. Crystallographic refinement details of thiophenol, selenophenol and their solid solutions

Data	Thiophenol	Selenophenol	5: 95 solid solution	9: 91 solid solution	25: 75 solid solution	43:57 solid solution
Formula	C_6H_6S	C_6H_6Se	$C_6H_6S_{0.95}Se_{0.05}$	$C_6H_6S_{0.91}Se_{0.09}$	$C_6H_6S_{0.75}Se_{0.25}$	$C_6H_6S_{0.57}Se_{0.43}$
Temperature (K)	90	90	90	90	90	90
Crystal system	Orthorhombic	Orthorhombic	Orthorhombic	Orthorhombic	Orthorhombic	Orthorhombic
Space group	*Pnab*	*Pnab*	*Pnab*	*Pnab*	*Pnab*	*Pnab*
a (Å)	7.191(1)	7.329(4)	7.191 (1)	7.193(2)	7.211(1)	7.262(2)
b (Å)	11.464(2)	11.226(5)	11.445(1)	11.425(3)	11.390 (2)	11.371(3)
c (Å)	13.815(2)	14.422(7)	13.854(1)	13.856(4)	13.971(2)	14.155(3)
α (°)	90	90	90	90	90	90
β (°)	90	90	90	90	90	90
γ (°)	90	90	90	90	90	90
Volume (Å^3)	1138.8(3)	1186.7(10)	1140.2(2)	1138.8(5)	1147.4(3)	1168.9(5)
No. of unique reflections	1122	1044	1125	1122	1132	1140
No. of parameters	67	49	70	70	70	70
$R_{\_all}$, $R_{\_obs}$	0.067,0.068	0.108, 0.085	0.078, 0.063	0.108, 0.078	0.066, 0.064	0.16, 0.082
wR_{2_all}, wR_{2_obs}	0.17,0.17	0.20, 0.20	0.15, 0.15	0.21, 0.20	0.15, 0.15	0.15, 0.13
$\Delta\rho_{max,min}$ (e Å^{-3})	0.39, -0.71	1.16, -1.49	0.34, -0.38	0.59, -0.50	0.43, -0.58	0.46, -0.46
GOF	1.29	1.35	1.23	1.16	1.39	1.08

Table S2. The intermolecular interactions in thiophenol and selenophenol

Crystal	D-H···A	D-H/Å	D···A/Å	H···A/ Å	∠D-H···A/°	symmetry
Thiophenol	S1···S1	3.580(2)				-x+ 1/2 ,+y,-z+1
	C2-H2···Cg1	0.92	3.586(5)	2.76	148	1/2 + x, 1/2 - y, 1/2 - z
	S1-H1···S1	1.32	4.224(2)	2.94	163	x – 1/2, - y + 1, + z
Selenophenol	Se1···Se1	3.756(2)				-x + 1/2,+y,-z+1
	C2-H2···Cg2	0.92	3.715(1)	2.86	151	1/2 + x, 3/2 - y, 1/2 - z
	Se1-H1···Se1	1.46	4.357(2)	3.05	148	x – 1/2, - y + 1, + z

Cg1 = centroid for the ring C1, C2, C3, C4, C5, C6; Cg2 = centroid for the ring C1, C2, C3, C4, C5, C6

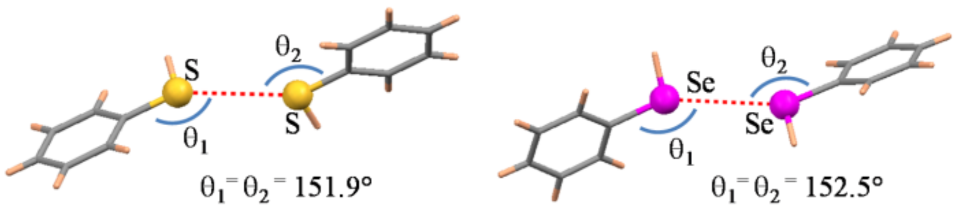

Figure S3. The homo-chalcogen interactions in thiophenol and selenophenol highlighting the ∠C–S···S angle.

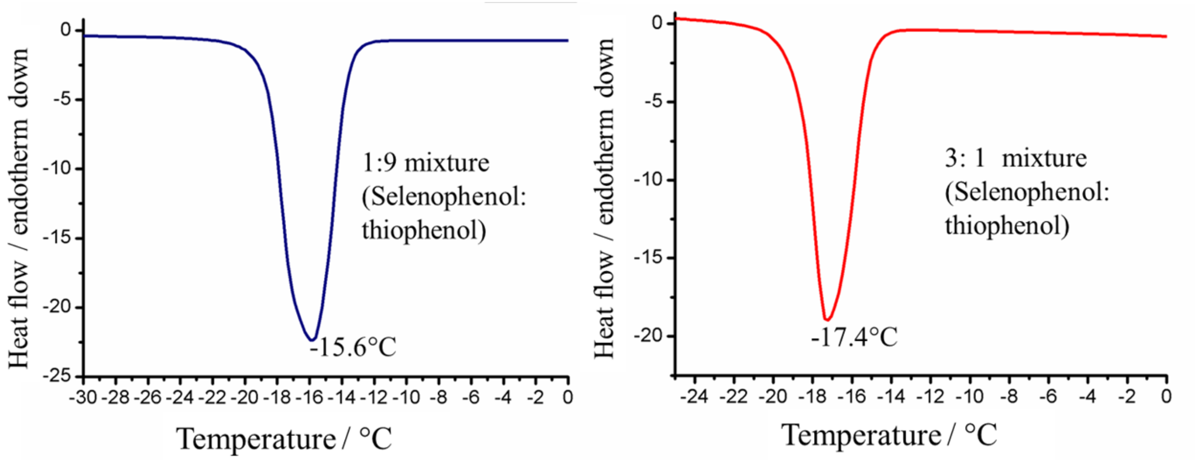

Figure S4. Endothermic peaks observed for the melting of alloy phases from differential scanning calorimetry (DSC).

3. Cambridge structural database analysis

There exist 7112 crystal structure entries in the CSD that have S···S contact distances less than 3.6 Å, the sum of van der Waals radii. The mean S···S contact distance was found to be 3.471 Å. Similarly, 1049 structures were found to exhibit Se···Se homochalcogen bonding with a mean contact distance of 3.605 Å (the sum of van der Waals radii being 3.8 Å). Hence, it should be noted that the observed contacts in thiophenol and selenophenol represent only weak or borderline cases of homo-chalcogen interactions despite the absence of any strong intermolecular hydrogen bonds in those structures. A search for the Se···S hetero-chalcogen interactions resulted in 253 hits with a mean Se···S contact distance of 3.560 Å.

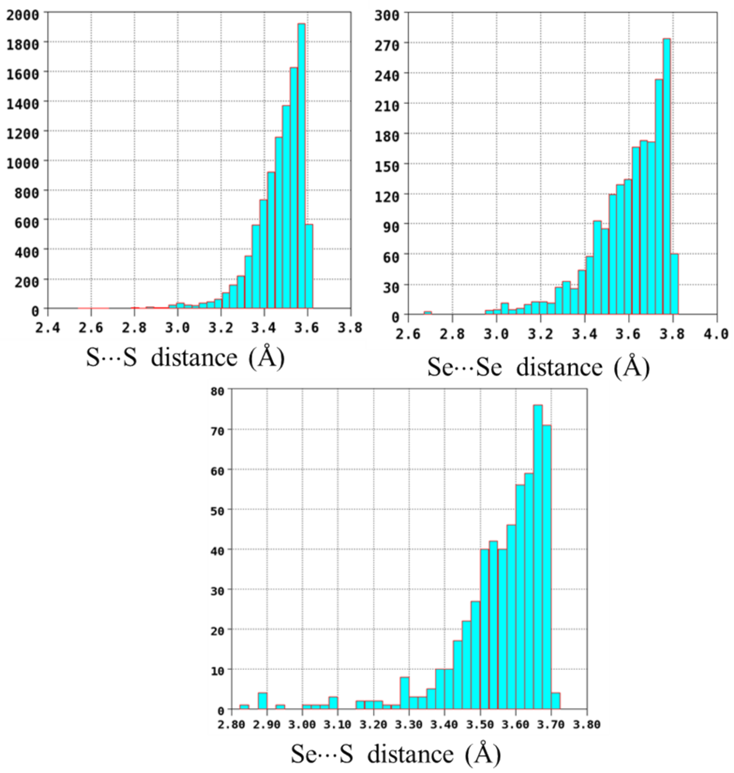

Figure S5. The distribution of various chalcogen bonding interactions in the CSD.

4. Hirshfeld surface analysis

A comparison of interaction contributions in terms of atom…atom contact surface area in the Hirshfeld surfaces of thiophenol and selenophenol shows that the analogues interactions in both structures exhibit “conservation of interaction proportions” as demonstrated by us earlier (S. P. Thomas, K. Shashiprabha, K. R. Vinutha, S. P. Nayak, K. Nagarajan and T. N. G. Row, *Cryst Growth Des*, 2014, **14**, 3758.).

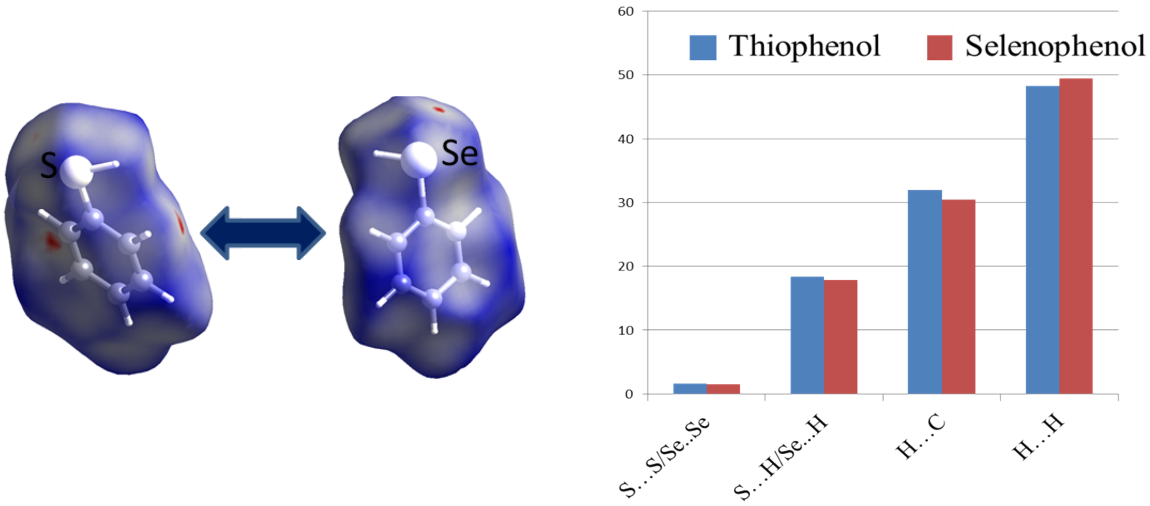

(a) (b)

Figure S6. (a) Hirshfeld d_{norm} surfaces depicting the isostructural features of intermolecular interactions in thiophenol and selenophenol and (b) the corresponding interaction contributions.

5. Energy framework calculations

The computational approach involves the following steps; (i) calculation of molecular wave function is performed at B3LYP/ 6-31G(d,p) level at crystalline geometry (with the X-H bond lengths normalized to neutron diffraction values), (ii) the density matrix for each molecule in the asymmetric unit is then subjected to crystallographic symmetry operations to generate corresponding density matrices for the neighbouring molecules (iii) the intermolecular electrostatic, repulsive, polarization, and dispersion terms for each molecular dimer are separately calculated and summed up to obtain the pairwise interaction energy values as,

$$E_{total} = E_{electrostatic} + E_{polarization} + E_{dispersion} + E_{repulsion} ,$$

(iv) Visualization of the molecular packing along with the obtained values of interaction energies between different molecular dimers, represented as cylinders joining the centres of mass of the molecules. The radius of the cylinder is plotted proportional to the value of interaction energy. Thus it provides a unique way to visualize the supramolecular architectures in crystal structures as tubular structures that could be termed as *energy frameworks,* representing relative strengths of molecular packing in different directions. Hence, a stronger interaction in a certain direction is represented as a thicker tube in the energy framework. (For details, see: a) M. J. Turner, S. Grabowsky, D. Jayatilaka and M. A. Spackman, *J. Phys. Chem. Lett.*, 2014, **5**, 4249; b) M. J. Turner, S. P. Thomas, M. W. Shi, D. Jayatilaka and M. A. Spackman, *Chem Commun*, 2015, **51**, 3735).

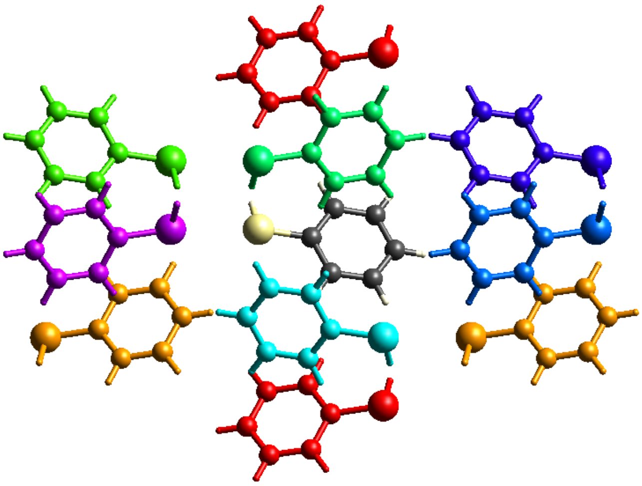

Figure S7. Energy colour coding for thiophenol, based on the distance and interaction energy between the central molecule and colour coded molecule (as given in table below).

	Symop	Dist.	Wavefunc.	Coul.	Polariz.	Disp.	Repul.	Total
🟥	x, y+1/2, -z+1/2	5.74	B3LYP/6-31G(d,p)	-2.7	-0.5	-8.4	3.3	-8.3
🟧	-x, -y+1/2, z+1/2	7.51	B3LYP/6-31G(d,p)	-2.5	-0.6	-5.5	5.6	-4.4
🟨	-x+1/2, y, -z	7.86	B3LYP/6-31G(d,p)	-0.2	-0.2	-5.8	1.1	-4.6
🟩	-x, -y, -z	7.77	B3LYP/6-31G(d,p)	-0.8	-0.6	-5.4	5.9	-2.4
🟩	x+1/2, -y, z	4.60	B3LYP/6-31G(d,p)	-11.1	-1.5	-19.9	19.1	-18.4
🟦	x+1/2, -y+1/2, -z+1/2	4.61	B3LYP/6-31G(d,p)	-3.6	-0.8	-17.9	9.4	-14.0
🟦	-x+1/2, y, -z	7.25	B3LYP/6-31G(d,p)	-0.1	-0.1	-4.8	0.5	-4.0
🟦	-x, -y, -z	7.24	B3LYP/6-31G(d,p)	-1.8	-0.3	-9.3	4.4	-7.3
🟪	-x+1/2, y, -z	7.78	B3LYP/6-31G(d,p)	-3.0	-0.3	-3.5	9.8	-0.6
🟪	-x+1/2, y, -z	8.34	B3LYP/6-31G(d,p)	1.1	-0.1	-0.8	0.0	0.5

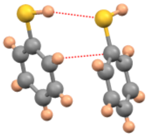	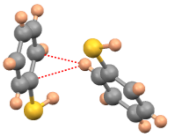	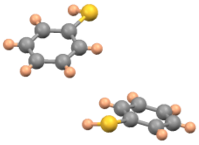	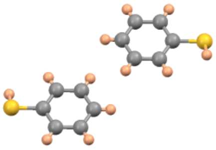
🟩 dimer I (-18.4)	🟦 dimer II (-14)	🟥 dimer III (-8.3)	🟦 dimer IV (-7.3)
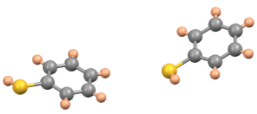	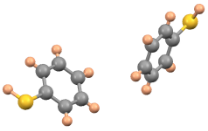	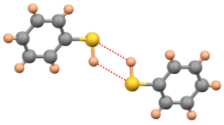	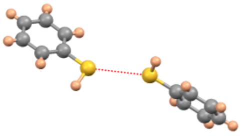
🟧 dimer V (-4.4)	🟦 dimer VI (-4)	🟩 dimer VII (-2.4)	🟪 dimer VIII (-0.6)

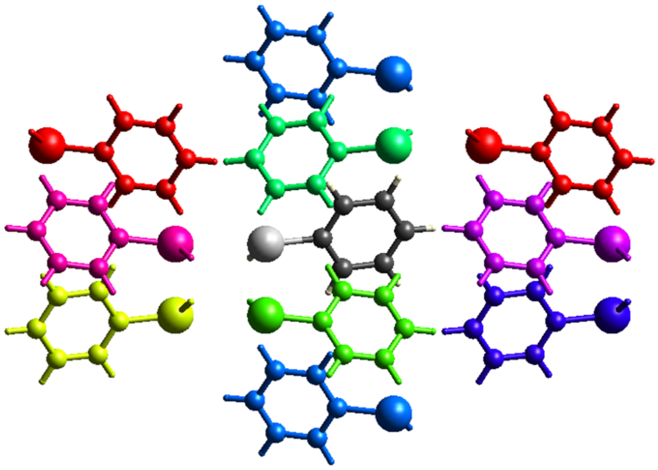

Figure S8. Energy colour coding for selenoophenol, based on the distance and interaction energy between the central molecule and colour coded molecule (as given in table below).

	Symop	Dist.	Wavefunc.	Coul.	Polariz.	Disp.	Repul.	Total
🟥	-x, -y+1/2, z+1/2	7.83	B3LYP/6-31G(d,p)	-2.7	-0.6	-7.1	5.4	-6.1
🟧	-x+1/2, y, -z	9.38	B3LYP/6-31G(d,p)	-0.1	-0.2	-5.2	1.0	-4.1
🟨	-x, -y, -z	6.77	B3LYP/6-31G(d,p)	-3.9	-0.4	-7.1	7.2	-6.1
🟩	x+1/2, -y, z	4.53	B3LYP/6-31G(d,p)	-7.6	-1.1	-22.0	16.7	-17.5
🟩	x+1/2, -y+1/2, -z+1/2	4.81	B3LYP/6-31G(d,p)	-2.9	-0.8	-19.5	9.9	-14.2
🟦	-x+1/2, y, -z	7.62	B3LYP/6-31G(d,p)	0.9	-0.1	-1.3	0.1	-0.1
🟦	x, y+1/2, -z+1/2	5.71	B3LYP/6-31G(d,p)	-3.7	-0.5	-9.9	3.7	-10.4
🟦	-x, -y, -z	8.71	B3LYP/6-31G(d,p)	-1.6	-0.3	-8.9	4.1	-6.9
🟪	-x+1/2, y, -z	8.73	B3LYP/6-31G(d,p)	-0.0	-0.1	-3.9	0.3	-3.2
🟪	-x+1/2, y, -z	6.81	B3LYP/6-31G(d,p)	-2.3	-0.2	-5.0	7.2	-2.5

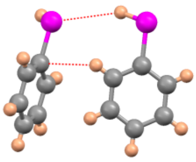	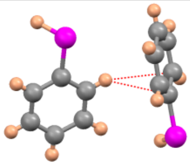	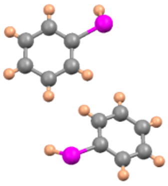	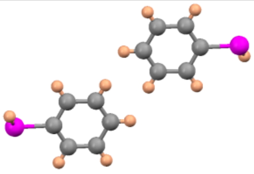
🟩 dimer I (-17.5)	🟩 dimer II (-14.2)	🟦 dimer III (-10.4)	🟦 dimer IV (-6.9)
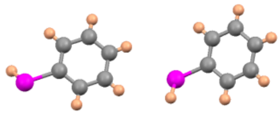	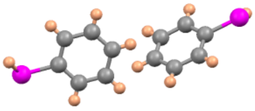	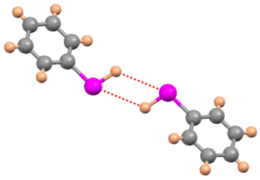	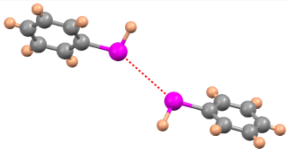
🟥 dimer V (-6.1)	🟧 dimer VI (-4.1)	🟨 dimer VII (-6.1)	🟪 dimer VIII (-3.2)

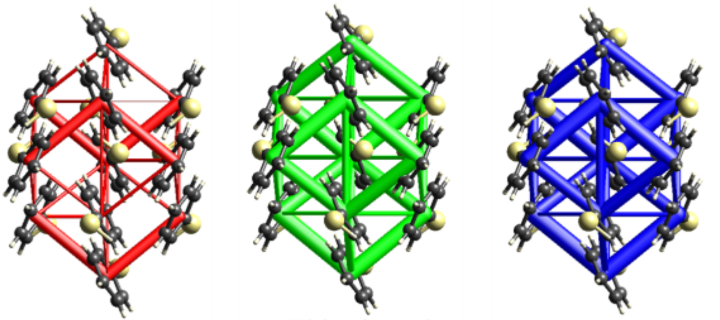

Thiophenol

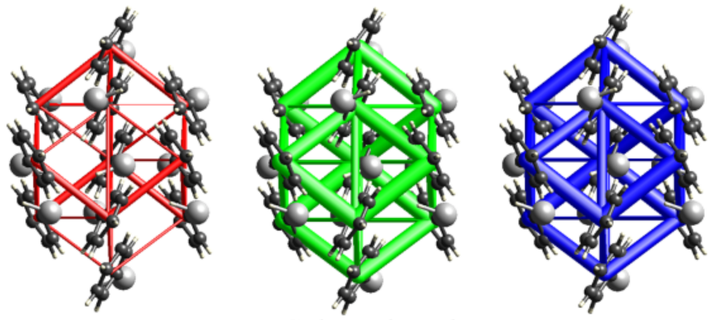

Selenophenol

Figure S9. Isostructurality of thiophenol and selenophenol manifested in their energy frameworks (viewed down *c*-axis). Red, green and blue frameworks correspond to electrostatic, dispersion and total energy contributions.

6. Theoretical charge density analysis

In order to quantitatively examine the structural features that lead to isostructurality in the crystals of thiophenol and selenophenol, theoretical charge density analyses have been carried out. Single point periodic quantum mechanical calculations at the B3LYP/TZVP level using the CRYSTAL09 package using the positional parameters obtained from the single crystal X-ray analysis. The shrinking factors and the reciprocal lattice vectors were set to 4 (with 30 k-points in irreducible Brillouin zone). ITOL1-ITOL4 = 8, and ITOL5 = 17 were set as the bielectronic Coulomb and exchange series values for the truncation parameter. The value for level shifter was set as 0.7 hartree/cycle. 10^{-6} Hartree was set as the SCF convergence limit.

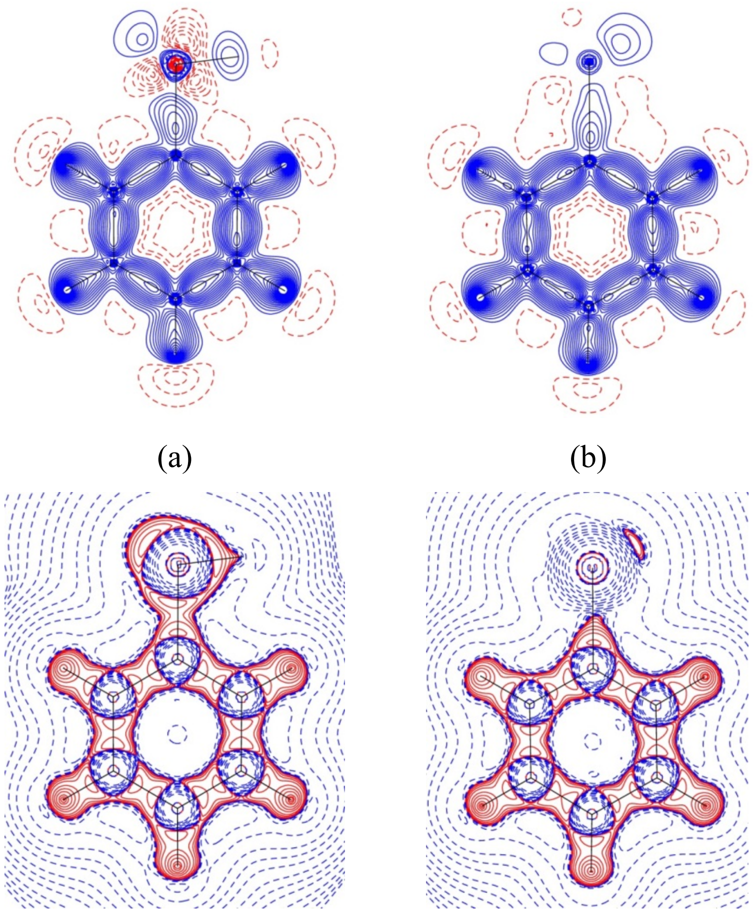

(a) (b)

(c) (d)

Figure S10. (a), (b) 2D static deformation density maps plotted with a contour level of ±0.05 eÅ^{-3} for thiophenol and selenophenol respectively. (c) and (d) corresponding Laplacian maps (drawn in logarithmic scale).

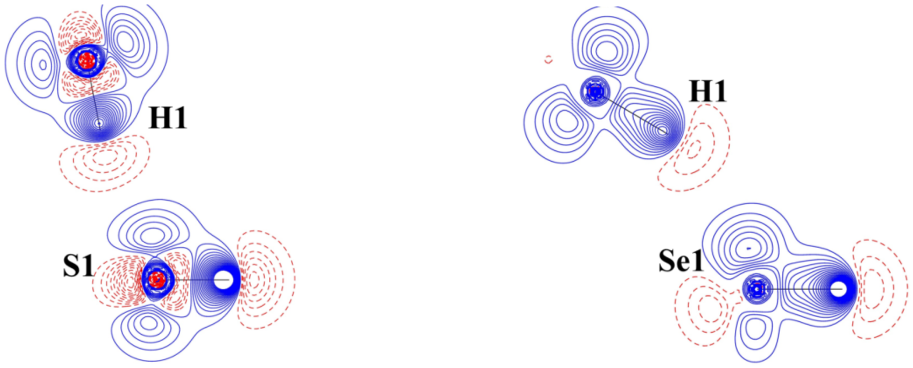

(a) (b)

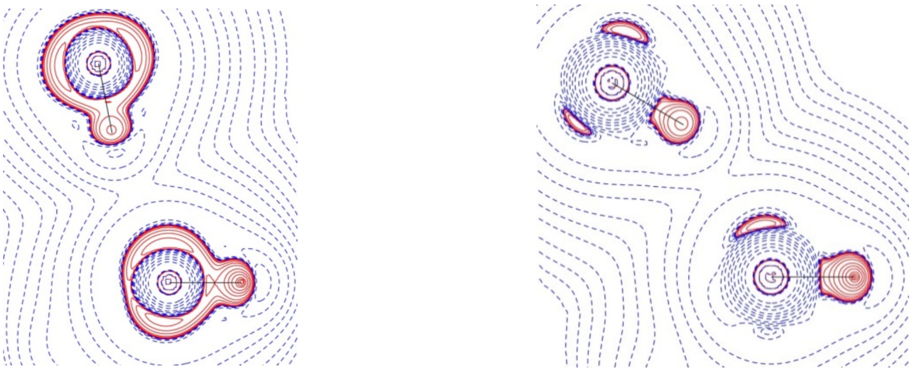

(c)

(d)

Figure S11. (a) and (b) 2D static deformation density maps plotted with a contour level of ±0.05 eÅ^{-3} for thiophenol and selenophenol respectively, for S–H···S and Se–H···Se hydrogen bond regions. (c) and (d) corresponding Laplacian maps (drawn in logarithmic scale).

Table S3. Charge density topological features of intermolecular interactions in thiophenol and selenophenol. Values of kinetic energy density (G) and potential energy density (V) are given in (kJmol^{-1}bohr^{-3}).

Interaction	**R_{ij}(Å)**	ρ **(eÅ^{-3})**	∇^{2}ρ **(eÅ^{-5})**	**G**	**V**	**G/│V│**
Thiophenol						
S–H···S	3.1078	0.02	0.4	7.7	-4.5	0.6
S···S	3.5837	0.07	0.6	14.6	-12.9	0.9
Selenophenol						
Se–H···Se	3.0830	0.03	0.5	10.0	-6.34	0.6
Se···Se	3.7562	0.05	0.5	11.2	-8.77	0.8
Alloy phase*						
S–H···Se	2.9060	0.06	0.12	5.04	-6.82	0.7
Se–H···S	3.0882	0.04	0.09	3.09	-3.73	0.8
S···Se	3.5125	0.04	0.12	3.63	-4.01	0.9

*The crystal structure of 43:57 phase is used for the calculation, as it is supposed to be representing a crude, average picture of the selenophenol-thiophenol interactions. The calculations were performed at B3LYP/6-311++G(d,p) level.

Table S4. Stockholder charges calculated from charge density models.

Thiophenol			
Atom	Stockholder charge	Atom	Stockholder charge
S1	-0.282	H1	0.091
C1	-0.055	H2	0.104
C2	-0.068	H3	0.075
C3	-0.020	H4	0.093
C4	-0.094	H5	0.087
C5	-0.044	H6	0.146
C6	-0.034		
Selenophenol			
Atom	Stockholder charge	Atom	Stockholder charge
Se1	-0.140	H1	0.083
C1	-0.060	H2	0.101
C2	-0.041	H3	0.073
C3	-0.052	H4	0.101
C4	-0.072	H5	0.052
C5	-0.060	H6	0.065
C6	-0.049		

The electrostatic potential (ESP) mapped on isoelectron density surface (for ρ= 0.5 e/Å^3) generated from the theoretical models are given in Figure S9. ESP maps show the electropositive regions (blue regions on the surface) corresponding to the σ-holes on both S and Se atoms. The features corresponding to the lone pair electrons on S and Se atoms are also evident as orange regions on the ESP surface. The esp maps are clearly in accordance with the 'sp^3 hybridization' states on both S and Se atoms.

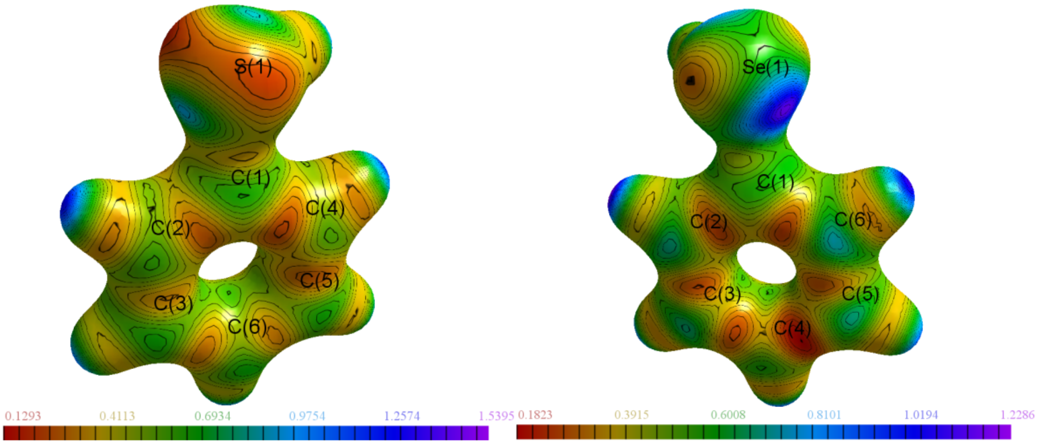

Figure S12. ESP mapped on isoelectron density surface (0.5 e/Å^3) on thiophenol and selenophenol.